SCHOOL OF MATERIALS AND MINERAL RESOURCES ENGINEERING

UNIVERSITI SAINS MALAYSIA

ELECTROCHEMICAL CHARACTERIZATION OF LITHIUM VANADIUM OXIDE ANODE WITH AGAR BINDER IN AQUEOUS RECHARGEABLE LITHIUM ION BATTERIES

By

JACQUELINE LEASE

Supervisor: Assoc. Prof Dr. Ahmad Azmin Bin Mohamad

Dissertation submitted in partial fulfillment

of the requirements for the degree of Bachelor of Engineering with Honours (Materials

Engineering)

Universiti Sains Malaysia

June 2018

DECLARATION

I hereby declare that I have conducted, completed the research and written the dissertation entitled **"Electrochemical Characterization of Lithium Vanadium Oxide Anode with Agar Binder in Aqueous Rechargeable Lithium Ion Batteries"**. I also declare that it has not been previously submitted for the award of any degree or diploma or other similar title of this for any other examining body or University.

Name of student   : Jacqueline Lease   Signature:

Date   : 12/6/2018

Witnessed by

Supervisor   : Assoc. Prof. Dr. Ahmad Azmin Bin Mohamad   Signature:

Date   : 12/6/2018

ACKNOWLEDGEMENTS

I would firstly like to express my sincere appreciation to my research supervisors, Associate Prof. Dr. Ahmad Azmin Mohamad for the academic guidance and constant encouragement throughout the project. I also want to thank him for sharing his knowledge and experiences through presentations and advices.

Furthermore, I want to express my deep gratitude to Ms. Nurul Nadia binti Mohd Zorkipli. She has lead me in the handling of experimental and material for this work. Besides, I'm appreciated for her readiness to freely share the knowledges and suggestions.

Apart from that, special thanks to all the technicians and supporting staffs especially Encik Azam, Encik Rashid, Encik Khairi, Encik Syafiq and Encik Azrul of School of Materials and Mineral Resources Engineering for their kind assistance and cooperation provided in completing my final year project.

Last but not least, I would like to express my deepest respect to my family and friends for their continuous support, understanding, and encouragement during my study, which enabled me complete this thesis.

TABLE OF CONTENTS

Contents   **Page**

LIST OF TABLES

LIST OF FIGURES

LIST OF ABBREVIATIONS

ARLB	Aqueous Rechargeable Lithium Batteries
C_{dl}	Capacitance of Double Layer
CD	Charge-Discharge
CE	Counter Electrode
CV	Cyclic Voltammetry
EDX	Energy-Dispersive X-Ray Spectroscopy
EIS	Electrochemical Impedance Spectroscopy
FESEM	Field Emission Scanning Electron Microscope
GEIS	Galvanostatic Electrochemical Impedance Spectroscopy
ICSD	Inorganic Crystal Structure Database
NWs	Nanowires
PEIS	Potentiostatic Electrochemical Impedance Spectroscopy
R_{ct}	Charge Transfer Resistance
R_s	Electrolyte Resistance
R_e	Electrolyte Resistance
RE	Reference Electrode
SCE	Saturated Calomel Electrode
SEM	Scanning Electron Microscopy
W	Warburg Impedance
WE	Working Electrode
XRD	X-ray Diffraction

LIST OF SYMBOLS

%   Percentage

o   Degree

Ω Ohm

$cm^2 s^{-1}$ Centimeter square per second

$mA\,h\,g^{-1}$ Mili-ampere hour per gram

$mV\,s^{-1}$ Milli-volt per second

^oC Degree Celsius

$^oC\,min^{-1}$ Degree Celcius per minute

A   Ampere

C   Current rate

cm   Centimeter

μm Micrometer

g   Gram

Hz   Hertz

V   Voltage

$W\,h\,kg^{-1}$ Watt-hour per kilogram

h   Hours

PENCIRIAN ELEKTROKIMIA ANOD LITIUM VANADUM OKSIDA DENGAN PENGIKAT AGAR DALAM BATERI BOLEH DICAS SEMULA BERDASARKAN ELEKTROLIT AKUES

ABSTRAK

Projek ini mengkaji kesan pengikat agar dalam anod litium vanadium oksida (LiV_3O_8) terhadap prestasi fizikal dan elektrokimia elektrod. Anod diperbuat daripada LiV_3O_8, grafin dan pengikat agar dalam nisbah 8:1:1 yang mana peratus agar akan dipelbagaikan. Elektrod aktif tersebut dikaji dalam sel-separuh. Analisis struktur mengesahkan bahawa struktur LiV_3O_8 dan grafin yang berlapis terbentuk. Pengikat agar dapat mengikat bahan aktif dan grafin dalam elektrod tersebut telah dibukti oleh analisis morfologi. Dengan kadar imbasan optimum iaitu 0.1 mV s^{-1}, pengikat agar 8% menunjukkan prestasi elektrod yang terbaik dalam kitaran voltammetri. Anod LiV_3O_8 ini juga mempunyai pekali penyebaran ion lithium yang tinggi, iaitu 1.315 x 10^{-6} dan 3.046 x 10^{-6} cm^2 s^{-1} bagi puncak anodik and kathodik, masing-masing. Keputusan rintangan pemindahan cas yang rendah daripada analisis impedan dalam anod menunjukkan kestabilan anod. Anod LiV_3O_8 juga menunjukkan permulaan kapasiti ion lithium bagi cas dan pelepasan iaitu 51.20 mA h g^{-1} dan 76.12 mA h g^{-1}. Prestasi kitaran yang baik dicapai dengan pengekalan kapasiti 84.10% selepas kitaran ke-10 pada kadar cas 2 C. Keputusan elektrokimia bagi anod LiV_3O_8 menunjukkan kemerosotan pada permulaan pencirian tetapi prestasi anode kembali stabil selepas kitaran ke-25. Kombinasi anode LiV_3O_8 dan pengikat agar menunjukkan keputusan yang baik dalam kajian ini.

ELECTROCHEMICAL CHARACTERIZATION OF LITHIUM VANADIUM OXIDE ANODE WITH AGAR BINDER IN AQUEOUS RECHARGEABLE LITHIUM ION BATTERIES

ABSTRACT

The objective of this research is to study the effect of agar binder in lithium vanadium oxide (LiV_3O_8) anode on electrochemical and physical performance of the electrode. LiV_3O_8, graphene and agar binder were used to prepare LiV_3O_8 electrode in 8:1:1 ratio with different percentage of agar binder. The working electrode allowed to be characterized as a half-cell setting for the characterization. The structural analysis confirmed that the layered structure of LiV_3O_8 and graphene were formed. The binder was also successfully bind the matrix of active material and graphene together based on the morphology analysis. With the optimum scan rate (0.1 mV s^{-1}) in cyclic voltammetry (CV), 8% agar electrode has the best performance. The high coefficient diffusion of lithium ions at 3.046 x 10^{-6} (anodic) and 1.315 x 10-6 cm^2 s^{-1} (cathodic) for the peaks were also further determined by CV characterization. Low charge transfer resistances from impedance analysis in the anode half-cell showed the stability of the anode. The capacity of the anode fading slowly upon cycling. Best scan rate in charge/discharge has shown to obtain desirable initial specific charge and discharge capacities which are 51.20 mA h g^{-1} and 76.12 mA h g^{-1}. A good cyclic performance with 84.1% capacity retention was obtained for 10 cycles at charge rate 2 C. Throughout the characterization, the anode will degrade at the initial cycles but return to stable after 25 cycles. LiV_3O_8 showed promising results when agar binder was added in this study.

CHAPTER 1

INTRODUCTION

1.1 Background of the study

Lithium-ion batteries (LIBs) are now widely utilized as the power source from portable electronics to electric vehicles. In comparison with non-aqueous lithium ion batteries, aqueous rechargeable lithium batteries (ARLB) have particular advantages including high ion conductivity, high rate capability, high power densities, inherent safety, environmental friendly and low cost (Liu *et al.*, 2011).

Lithium vanadium oxide (LiV_3O_8) is one of the typical used in LIBs. LiV_3O_8 is a cathode material for non-aqueous rechargeable lithium batteries while it is also an anode material for aqueous rechargeable lithium batteries. LiV_3O_8 has cycle stability, high specific energy and the facile preparation has a layered structure with two basic structural units of octahedral and distorted trigonal bi-pyramid. The lithium ions in octahedral sites link to the V_3O_8 layer through strong ionic bonds, which makes the crystal structure of LiV_3O_8 stable during the intercalation or deintercalation processes (Heli, Yadegari and Jabbari, 2011).

The electrolyte in battery acts as the ionic conductor and electronic barrier for the anode. During the cell reaction, the electrolyte should maintain its mechanical, chemical and electrochemical inertness toward electrodes. Generally, lithium nitride ($LiNO_3$) and lithium sulphate ($LiSO_4$) are utilized in aqueous rechargeable lithium batteries (Li, 2016).

Polymer binder is also a material that play a critical role to maintain the integrity of the active electrode. Binder used for bridging the active materials and current collector while it will control the volumetric change of electrodes. Poly-vinylidene fluoride (PVDF) is a typical binder that used in organic LIBs. It shows good chemical resistance properties in organic solvent which can prevent delamination of the active metal.

However, PVDF has its own weakness in the LIBs field, especially for ionic liquid-based electrolytes. It tends to swell in ionic electrolyte which cause the active metal split from the current collector. Delamination of active mass will shorten the battery life, so it is important to choose the correct binder with correct ratio (Barsykov and Khomenko, 2010). Therefore, researchers have to search for new binders or study the new combination of PVDF with other materials in order to overcome the problem.

1.2 Problem Statement

In order to improve the performance of LIBs, binder plays an essential role. PVDF is the common binder materials that usually used in Li-ion batteries. PVDF has good adhesion property to link the current collectors and also the active materials. But, it can easily undergoes degradation due to the formation of LiF and $C=CF^-$ after the intercalation/de-intercalation of Li ion in the electrolyte. Recently, PVDF faced a safety issue. Exothermal reaction of PVDF and Li will cause self-heating and thermal runaway. Besides, PVDF which mixes with N-methyl-pyrrolidone is not environmental friendly and pricey (Lu *et al.*, 2016).

Thus, bio-polymer binder gets a big attention from the public. Bio-polymer binders such as chitosan, sodium carboxymethyl cellulose (Na-CMC), guar gam (GG), gum arabic (GA), xanthan gum (XG), agar (Ag) and carrageenan (CAR) can use as bio-polymer binder in aqueous lithium ion battery. Agar is chosen as the binder in the anode for this study because of it good adhesion properties (Cuesta *et al.*, 2015). However, there has not been previous research on the effect of agar binder in LiV_3O_8 anode and the characterization of LiV_3O_8 anode with agar binder is seldom been done before. Thus, there exists a compelling factor in investigating the interaction of agar binder, graphene and LiV_3O_8.

1.3 Objectives

The objectives of this study are:

i. To prepare the anode (LiV_3O_8-Graphene-Agar) for different agar binder percentages to get the optimum ratio.

ii. To determine the cycle behaviour, diffusion coefficient, electrochemical impedance and also the battery performance of the LiV_3O_8 anode.

iii. To characterize the degradation behaviour of LiV_3O_8 anode using structural, morphology and elemental analysis.

1.4 Scope of Work

Some of the scope of the research which has been carried out in this study is briefly outlined here. In this chapter, a general background and major problems associated with lithium-ion battery electrode binder are presented. Possible approaches for improving battery performance and the objectives of this study are also presented.

In Chapter 2, a comprehensive literature review on lithium-ion battery and the components, especially with respect to the role of electrode materials and their possible synthesis techniques are discussed. Chapter 3 discusses the overall experimental methods used in this study and also the details of the materials and chemicals used to synthesize the LiV_3O_8 electrode.

Discussions and results of the electrochemical characterization such as cyclic voltammetry, charge/discharge characterization, electrochemical impedance spectroscopy, x-ray diffraction, scanning electron microscopy and energy dispersive x-ray spectroscopy are presents in Chapter 4. For the last chapter (Chapter 5), it will summarize the results of this thesis and provides some indications for further research work related to electrode materials.

CHAPTER 2

LITERATURE REVIEW

2.1 Introduction

In this chapter, basic aspects pertaining to the key components of lithium-ion batteries was discussed. The brief introduction to battery materials is confined to LiV_3O_8 anode, graphene, agar binder and electrolyte, aiming to facilitate the discussions to be given in the following chapters. Then, various characterization techniques used in this study, specifically cyclic voltammetry (CV), electrochemical impedance spectroscopy (EIS), charge-discharge (CD), x-ray diffraction (XRD), scanning electron microscopy (SEM) and energy-dispersive x-ray spectroscopy (EDX).

2.1.1 Lithium Ion Batteries

Lithium Ion Batteries (LIBs) are secondary batteries where charging and discharging can happen. Lithium ions move from cathode to anode in the discharge process while lithium ions move from anode to cathode again to recover the original places upon recharging. The lithium ion battery is better than the lithium primary battery where recharging is impossible in primary battery (Shin *et al.*, 2015).

Theoretically, electrodes with a working potential between 3 and 4 V (vs. Li^+/Li) can be used as cathode and electrodes with a working potential between 2 and 3 V (vs. Li^+/Li) is chosen as anode. The potential table comparing with the stable potential window (vs. SHE) of water and working potential (vs. Li^+/Li, or Na^+/Na) of representative electrode materials as oxides, poly-anionic, and other compounds on the same potential scale (Table 2.1). Special caution should be taken in materials selection

in order to prevent water decomposition. pH value is the factor that affect the H_2 evolution potential and O_2 evolution potential (Liu *et al.*, 2017).

Table 2.1: Comparison between various aqueous rechargeable lithium ion batteries

Anode	Cathode	Electrolyte	Working Potential (V)	Capacity Retention (%)	Initial Capacity ($mAhg^{-1}$)	Reference
$LiFePO_4/C$	LiV_3O_8	9 M $LiNO_3$	0-0.8	~91.8% at 10 C	90	(Zhao *et al.*, 2011)
LiV_3O_8	$LiMn_{0.6}Fe_{0.4}PO_4$	5 M $LiNO_3$	0-1.4	90% at 0.1 C	71.30	(Zhao *et al.*, 2015)
$LiMn_2O_4$	AC	0.5 M Li_2SO_4	0-1.8	~100%	110	(Zhu *et al.*, 2016)
$LiMn_2O_4$ nanochains	AC	0.5 M Li_2SO_4	0-1.8	~112%	110	(Peng *et al.*, 2013)
$LiMn_2O_4$ nanotubes	PPy/MoO_3	0.5 M Li_2SO_4	0-1.95	~90%	~88	(Zhou *et al.*, 2010)
$LiCoO_2$	Li	0.5 M Li_2SO_4	3.5-4.3	N.A.	~465	(Lecce *et al.*, 2018)

Various control parameter and processes in battery making cause the battery perform differently. Even same battery manufacturer, it will perform differently depending on what they are optimized for. There are many factors to consider when choosing a battery cell. Li ion and metal have smaller size and light weight properties if compared to others (Figure 2.1).
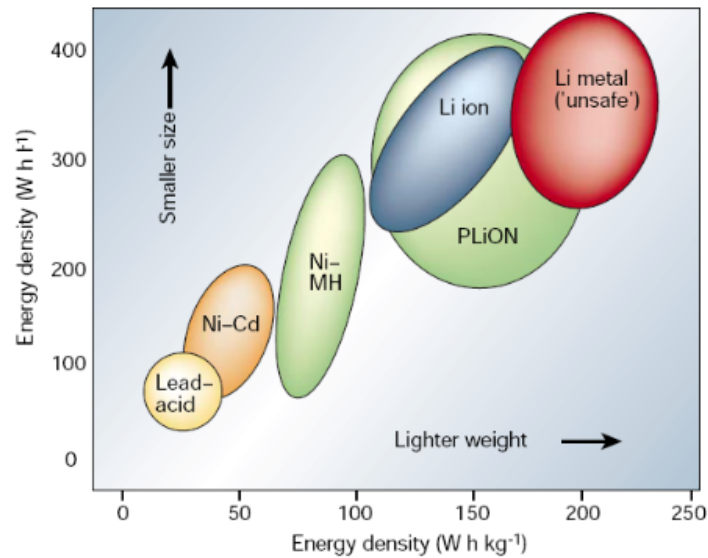
Figure 2.1: Comparison of the different battery materials based on volumetric and gravimetric energy density (Zhang, 2015)

In 1994, LIBs with an aqueous electrolyte was developed by Dahn's group. In that case, $LiMn_2O_4$ acts as cathode and VO_2 acts as anode. The aqueous electrolyte used consist of 5 M $LiNO_3$ in 0.001 M LiOH. The results showed the specific energy density of the aqueous rechargeable lithium-ion batteries (ARLB) was 75 W h kg^{-1} and it has a low cycling life. Although ARLB has lower performance than the conventional LIBs, it can solve the cost and safety issues (Zheng et $al.$, 2016).

2.1.1.1 Basics of Lithium Ion Batteries

Lithium ion battery is a device that can stored electrical energy in the form of chemical energy. It will convert the chemical energy into electricity. Three main components of the LIBs are cathode, anode and electrolyte (Figure 2.2) (Nitta and Yushin, 2013). Negative electrode is normally an electron donor group which is anode while positive electrode is an electron acceptor which is cathode. Anode electrochemically oxidized and releases electron during discharging. This electron moves through the outer circuit to the cathode which accepts electron (Whittingham, 2008).
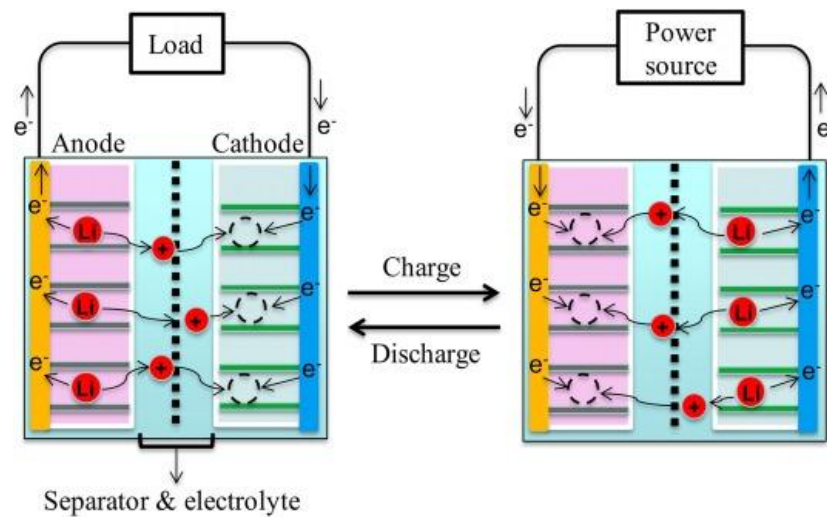
Figure 2.2: Schematic of lithium ion battery operation (Whittingham, 2008)

2.1.2 Aqueous Rechargeable Lithium Batteries

Aqueous rechargeable lithium batteries (ARLBs) were invented in 1994. It is getting popular due to its benefits such as low capital investment, high reliability and good safety. ARLBs use lithium active materials as electrode, current collect and aqueous electrolytes in the system. In addition, they can present very good cycling performance and super-fast charge performance. However, there are several experiments have been conducted on the anode materials, the performance lower as expected. Its main disadvantage is the energy density is still lower than conventional lithium ion batteries due to the narrow electrochemical window of water (Wang *et al.*, 2013).

If anode materials of lower redox potentials can be stable in aqueous electrolytes, high energy density systems are practicable in ARLB. Kohler *et al.* mentioned that oxides represent a novel material of high capacity materials which can be used in ARLB. Attention has been paid to vanadium oxides as a promising anode for ARLB. For instance, an ARLB based on LiV_3O_8 as anode with various kind of bio-polymer binder in aqueous electrolyte was successfully developed. (Zheng *et al.*, 2016).

2.1.3 Lithium Vanadium Oxide (LiV_3O_8) Anode

In Li ion battery, only a few compounds with proper redox potential are available for anode materials. LiV_3O_8 is chosen because of its advantages. The structure reversibility of LiV_3O_8 is much better than that of V_2O_5, so it has good potential to obtain stable capacity during long cycling (Liu *et al.*, 2011). Moreover, it has high specific capacity and layered structure that can enhance the properties of lithium ion battery. Lithium ions generally occupy the octahedral sites. However, extra lithium ions that intercalate into the host compound may enter the tetrahedral sites. The lithium ions

in octahedral sites link to the V_3O_8 layer through strong ionic bonds, which makes the crystal structure of LiV_3O_8 stable during the intercalation or de-intercalation processes (Heli, Yadegari and Jabbari, 2011)

Kohler et $al.$ (2000) have characterized LiV_3O_8 as anode material for aqueous lithium batteries. During charging and discharging, the potentials will change slow as the process is on-going. Selection of intercalation materials which intercalates and de-intercalates Li ion at the corresponding potential is also a vital step to obtain high performance of ARLB (Figure 2.3). The specific discharge capacity of LiV_3O_8 anode is between 40 and 45 mA h g^{-1} without formation of plateau. The performance of LiV_3O_8 decreased sharply at high potential of 1.9 V indicates that LiV_3O_8 is less stable in aqueous electrolytes. Degradation behaviour of electrode occurs due to the chemical reactions between the electrolyte and electrode (Zheng et $al.$, 2016).

Moreover, Wang et $al.$ (2016) have found a cyclic performance with capacity retention of 29.5. The specific capacity of LiV_3O_8 is 20.2 mA h g^{-1} after 220 cycles. Besides, the discharge capacity can remain above 10 mA h g^{-1} after 400 cycles. LiV_3O_8 has a very stable layered structure due to the existing Li^+ ion between the layers of VO_6 octahedral and VO_5 trigonal bipyramids (Figure 2.3). Every materials have its pro and con. There are side reactions causing the capacity fading in LiV_3O_8 as well as the side reaction will happen for the ion and the electrolyte. The potential electrode materials can be determined as well in order to improve aqueous rechargeable lithium-ion batteries' performance (Figure 2.4).
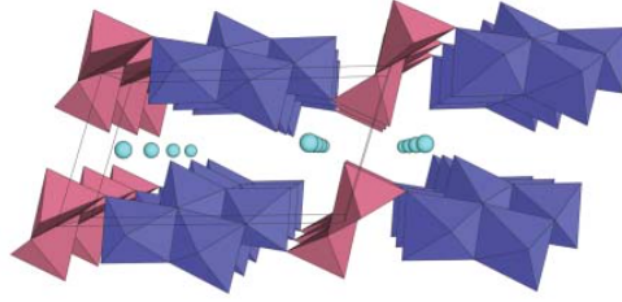
Figure 2.3: Schematic diagram of the structures of LiV$_3$O$_8$ layered. VO$_5$ square pyramids are pink, VO$_6$ octahedra are purple, and lithium atoms are blue (Whittingham *et al.*, 2005)
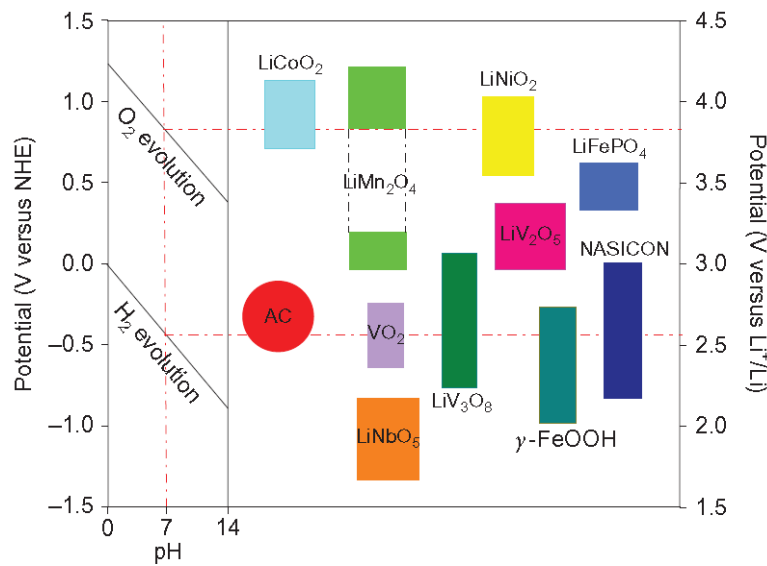
Figure 2.4: The potential electrode materials which could be used for aqueous rechargeable lithium-ion batteries (Luo *et al.*, 2010)

2.1.3.1 Synthesis of LiV$_3$O$_8$ - Sol Gel Method

Crystal structure and electrochemical performances of LiV$_3$O$_8$ are significantly influenced by synthesized routes and processing parameters. There are kinds of techniques are utilized to prepare the LiV$_3$O$_8$ materials such as sol–gel method, spray pyrolysis process, hydrothermal reaction, freeze drying technique and solid-state

11

reaction as well as combustion synthesis. Based on Zhong *et al.* (2011) among these methods, sol–gel process could be the excellent method for the synthesis of active materials due to its unique advantages in the synthesis of oxide materials.

Sol–gel method has been extensively used to synthesize electrode. It has many good points to be chosen as synthesize technique such as it requires low synthesis temperature, produces high homogeneous structure, good electrochemical property and high purity of the synthesized product. Many works have been done to fabricate LiV_3O_8 material by using sol–gel methods in which citric acid was mostly selected as chelating agent. In sol–gel process, it will take several hours to finish the reaction of sol formation (Wang *et al.*, 2012).

In addition, some researchers decided to choose sol–gel process to synthesize the LiV_3O_8 electrode material by using citric acid as chelating agents. The effects of usage of citric acid and sintered temperature on the preparation of LiV_3O_8 has been studied. The morphology analysis, electrochemical performance and phase composition of the active materials were also studied to know the properties of the materials. Oxalic acid is another popular chelating agent which selected in this research as well (Wang *et al.*, 2012).

Based on Pan *et al.* (2011) and Liang *et al.*(2013), LiV_3O_8 calcined at 500 °C for 5 hours demonstrated the best specific capacity. An initial specific discharge capacity of 260 mA h g^{-1} and excellent capacity retention (99 percent) at 100 mA g^{-1}. After 100 cycles, a specific discharge capacity of 262 mA h g^{-1} was retained, which is among the best performances ever reported. Calcination temperature can be fixed to improve the battery performance as well.

2.2 Electrochemical Characterization of LiV₃O₈ Anode

2.2.1 Cyclic Voltammetry: Redox and Diffusion Coefficient of Li⁺

Cyclic voltammetry (CV) is as widely used technique for investigating the thermodynamics and kinetics of electron transfer at the electrode-electrolyte interface. In a CV characterization of LiV_3O_8, the working electrode potential is ramped linearly versus time, and the corresponding current is recorded. The CV curve is a function of current value versus potential. When an electrochemical redox reaction occurs, a distinct peak will be generated at both the forward and reverse scans due to the current changes. The scan rate is a function of time versus the change of potential, which is the main parameter for CV measurements (Zhang, 2015).

The cyclic voltammetry curves of LiV_3O_8 nanowires, $LiMn_2O_4$ and steel mesh are performed using the saturated $LiNO_3$ electrolyte (Figure 2.5). The hydrogen and oxygen evolutions occurs at about 1.2 and 1.8 V vs. SCE (saturated calomel electrode) due to over-potentials. Only a pair of well-defined redox peaks is observed for the LiV_3O_8 nanowire electrode. The anodic peak is centered at 0.093 V, while the cathodic peak is centered at 0.445 V vs. SCE.

This is due to the intercalation and de-intercalation of Li^+ ion into or from the layered LiV_3O_8 structure, which is in good agreement with the behaviours of LiV_3O_8 electrodes in non-aqueous electrolytes. The evolution of hydrogen in the aqueous electrolyte occurs at much lower potential, about 1.2 V, suggesting that LiV_3O_8 nanowires electrode is very stable during the Li^+ de-insertion or insertion processes (Zhang, 2015).

The right curve in Figure 2.5 (a) shows the cyclic voltammetry curve of $LiMn_2O_4$. The anodic and cathodic peaks of the lower potential pair occur at 0.98 and 0.73 V vs. SCE. Meanwhile, for the higher potential pair are showed at 1.12 and 0.87 V

vs. SCE. Based on the above discussion, an ARLB can be prepared by using the LiV_3O_8 nanowire and $LiMn_2O_4$, as the negative and positive electrodes. (Liu *et al.*, 2015). They tends to give good performance in this battery system. Cheap aqueous electrolyte like saturated $LiNO_3$ solution can be used as electrolyte. So, the safety issue which caused by organic electrolyte can be completely avoided. Few examples of cyclic voltammogram of LiV_3O_8 were illustrated in Figure 2.6.
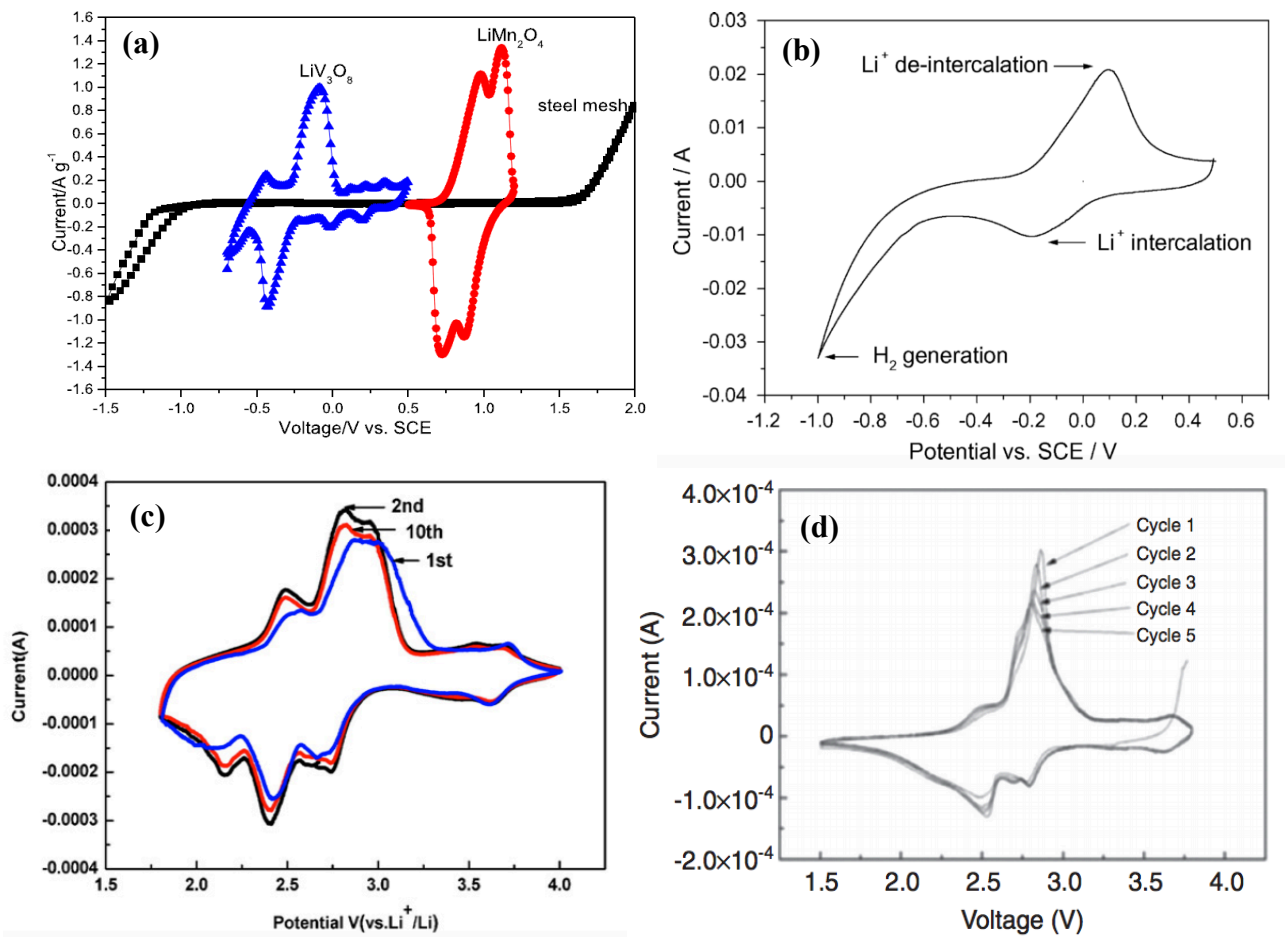
Figure 2.5: Cyclic voltammograms of (a) LiV_3O_8 and $LiMn_2O_4$ at 1 mV s^{-1} (Liu *et al.*, 2015), (b) LiV_3O_8 in saturated $LiNO_3$ aqueous electrolyte (Wang *et al.*, 2007), (c) LiV_3O_8 for 10 cycles (Xiong *et al.*, 2012) and (d) nanostructured LiV_3O_8 thin film (Liu *et al.*, 2014)

Scan rate in CV is pretty essential to obtain a well-defined curve. Indirectly, it will affect the behaviour and the performance of the battery electrode. With the increase of the scan rate, the peak current becomes broader and polarization will occur (Liu *et al.*, 2011). For instance, cyclic voltammograms of the LiV_3O_8 electrode in 0.5 M Li_2SO_4 aqueous electrolyte at different scan rates are shown in Figure 2.6 (a).

There is a pair of redox peaks between -0.6 V and 0.2 V (versus SCE) at various scan rates, corresponding to the intercalation and de-intercalation of lithium ions into and from the LiV_3O_8 anode. Figure 2.6 (b) presented the different scan rate of $LiMn_{0.75}Fe_{0.25}PO_4$ electrodes. It is also showed that as the scan rate increases, the separation between the cathodic and anodic increases. The significant peaks will combine to form a large peak and sometimes no peak will occur due to high charge rate (Kim *et al.*, 2016).

Apart from that, anodic and cathodic peak currents linearly depend on the square root of the scan rate. This linear graph indicates that the intercalation/deintercalation process is controlled by Li^+ diffusion in the host material. Using the slopes of the linear graph and on the basis of the Randles-Sevcik equation in equation 2.1, diffusion coefficient of Li^+ ion (D_{Li}) can be calculated. The average value of D_{Li} into the nanosheets of LiV_3O_8 is obtained as 3.39×10^{-10} $cm^2\,s^{-1}$ (Heli, Yadegari and Jabbari, 2011).

$$I_p = 2.69 \times 105An^{2/3}c_oD^{1/2}v^{1/2} \tag{2.1}$$

where I_p, n, A, and v are the peak current, number of exchanged electrons, surface area of the electrode and scan rate. D_{Li} is the chemical diffusion coefficient of lithium ion, while C_{Li} is the bulk concentration of lithium ion.
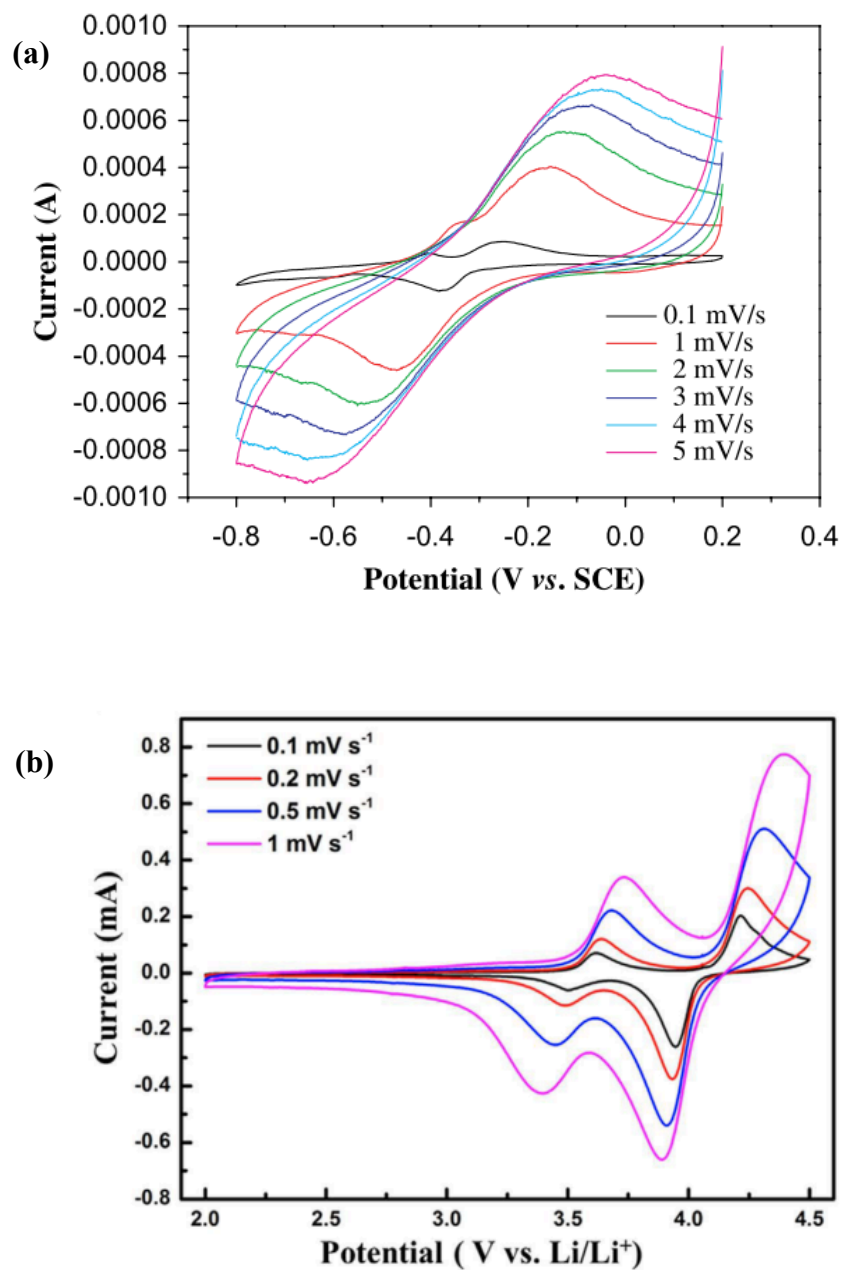
Figure 2.6: The cyclic voltammograms of (a) LiV_3O_8 at various scan rates using SCE as the reference electrode (Liu *et al.*, 2011) and (b) $LiMn_{0.75}Fe_{0.25}PO_4$ obtained at scan rates of 0.1, 0.2, 0.5, and 1.0 mV s^{-1} (Kim *et al.*, 2016)

2.2.2 Electrochemical Impedance Spectrometry

Electrochemical impedance spectroscopy (EIS) is used for characterizing the energy storage and dissipation properties of electrochemical systems in the LiV_3O_8 electrode. EIS measures the impedance of a system over a range of frequencies, which can be carried out in potentiostaic (PEIS) or galvanostatic (GEIS) mode. A common type EIS spectrum consists of a low-frequency semicircle and a high-frequency tail. The PEIS are conducted by using a sine wave around a potential (V) (Ribeiro *et al.*, 2015).

The potential can be set to a fixed value or a value relative to the working electrode equilibrium potential over a range of frequencies. A typical PEIS consists of a low frequency semicircle related to the kinetic process and a high-frequency tail resulting from the diffusion process. Usually, the high-frequency tail for the LIB system has a 45° angle. The GEIS is similar to the PEIS. The only difference is that the current is controlled instead of the potential (Zia and Mukhopadhyay, 2016). The corresponding equivalent circuit of EIS curve is showed in Figure 2.7. R_e is the uncompensated resistance; R_{ct} is the charge transfer resistance; C_{dl} is constant phase angle element and W is the Warburg impedance.
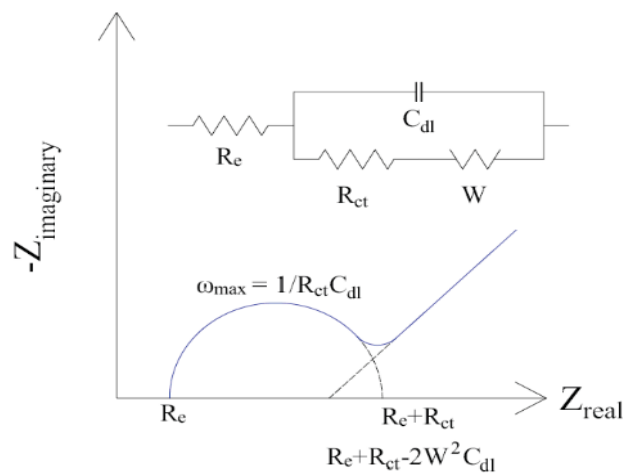

Figure 2.7: Typical equivalent circuit for LIBs (Zia and Mukhopadhyay, 2016)

Based on the Liu *et al.* (2015), the LiV₃O₈ electrode in 0.5 M Li₂SO₄ solution show that the Nyquist plot consists of three parts (Figure 2.8 (a)). There are an arc in the high frequency range, an inclining line in the low frequency range and a transitional area between the high frequency and the low frequency. In an electrochemical system, the resistance includes R_Ω from the resistance of the electrolyte, C_{dl} from the charge at the interface, Z_f due to the charge transfer and a diffusion resistance of materials during the redox reactions, R_{ct}. During the polarization at alternative current, a new resistance Z_w should be considered due to the periodic change of the concentration of the chemicals.
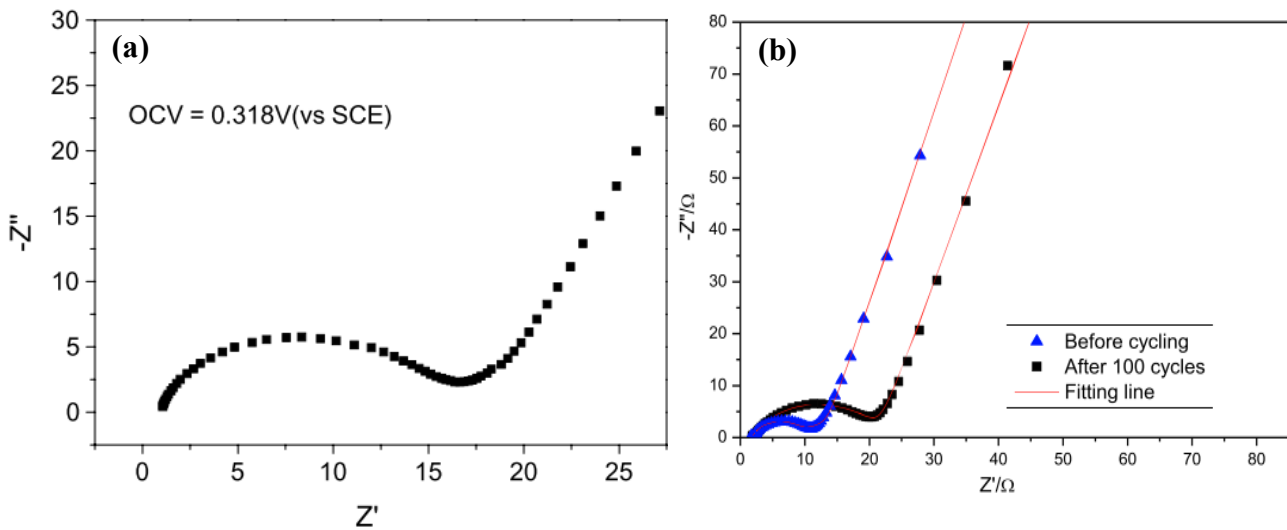
Figure 2.8: Nyquist plot of (a) the LiV₃O₈ at the open circuit voltage (Liu *et al.,* 2015) and (b) the LiV₃O₈ before cycling and after 100 cycles (Liu *et al.*, 2015)

The impedance will increase as the number of cycle increases. Figure 2.8 (b) shows the impedances gradually increases upon further cycling. Sometimes, the impedance will decrease at the beginning of the cycling. Decreasing of impedance in the initial cycling stage was likely due to the activation of the electrode surface. After

few cycles, the impedance results continuously increase due to the formation and growth of the surface layer on the electrode, which develop polarization effect (Jiao *et al.*, 2008).

2.2.3 Charge-Discharge

The capacity and cycling stability of the LiV_3O_8 materials were studied using galvanostatic charge-discharge tests in a constant current mode. The discharge/charge capacity (Q) can be calculated based on the discharge/charge time according to the formula $Q = I \times t$, where I is the current and t is the time. The rate capability of these electrodes can also be tested by setting up varying current densities applied over a number of cycles (Zhang, 2015).

A charge-discharge (CD) analysis was performed on the LiV_3O_8 electrode in 1 M Li_2SO_4 electrolyte (Kohler *et al.,* 2000). The specific discharge capacity of electrode was characterized at a cut-off potential of 0.5 V and 2 V (Figure 2.9). The battery systems achieved higher charge capacity than discharge capacity. The charge capacity is 70 mA h g^{-1} while the discharge capacity is 45 mA h g^{-1}.
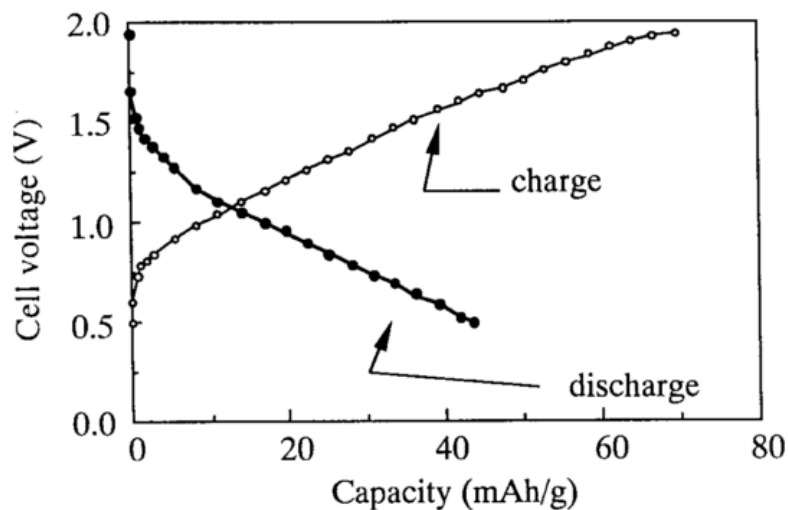

Figure 2.9: Charge/discharge curve of LiV_3O_8 at 1 mA/cm^2 (Kohler *et al.,* 2000)

The electrochemical performance of LiV_3O_8 nanowires/$LiMn_2O_4$ ARLB in the saturated $LiNO_3$ electrolyte at 150 mA g^{-1} was presented (Figure 2.10). It can be found that the initial charge capacity of the full system is 181.0 mA h g^{-1}, which is much larger than the discharge capacity (103.9 mA h g^{-1}). Furthermore, the coulombic efficiency at the first cycle is obtained, which is only 57.4%. This performance is indicating the existence of irreversible phase transformation and intercalation sites in the first cycle (Liu *et al.*, 2015).

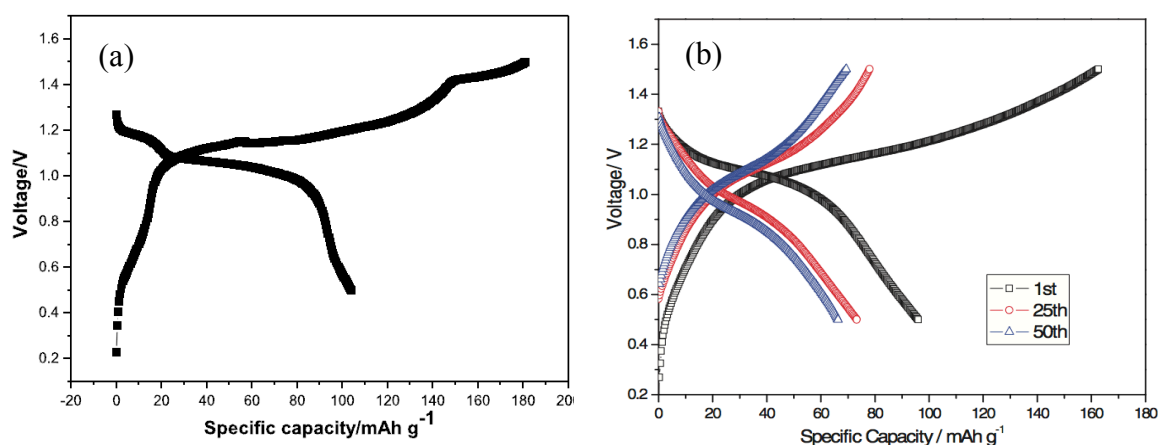Figure 2.10: Initial charge/discharge profiles of LiV_3O_8/$LiMn_2O_4$ aqueous rechargeable lithium battery at a current density of (a) 150 mA g^{-1} for one cycle (Liu *et al.*, 2015) and (b) 300 mA g^{-1} for 50 cycles (Liu *et al.*, 2012)

2.3 Physical Characterization of LiV_3O_8 Anode

2.3.1 Structural Properties

X-ray diffraction (XRD) is widely used for the identification of crystalline structures and phases of the LiV_3O_8 anode. In Figure 2.11, the significant peak of LiV_3O_8 electrode at about 2θ =13.9° is indexed to the (100) planes. (100) planes in LiV_3O_8 electrode indicating the layered structure of LiV_3O_8. The layers consist of VO_6 octahedron and VO_5 trigonal bipyramids, which share the corners in octahedral. Li^+ ions insertion and extraction in between these layers.

The diffraction peak for the (100) planes is the sharpest suggesting that the layers of VO_n polyhedral have a preferred orientation along [100] direction (Liu *et al.*, 2011). The figure 2.7 (a) is the guideline which LiV_3O_8 calcined at 550°C for 5 h while various temperature of calcination of LiV_3O_8 is showed in Figure 2.7 (b).
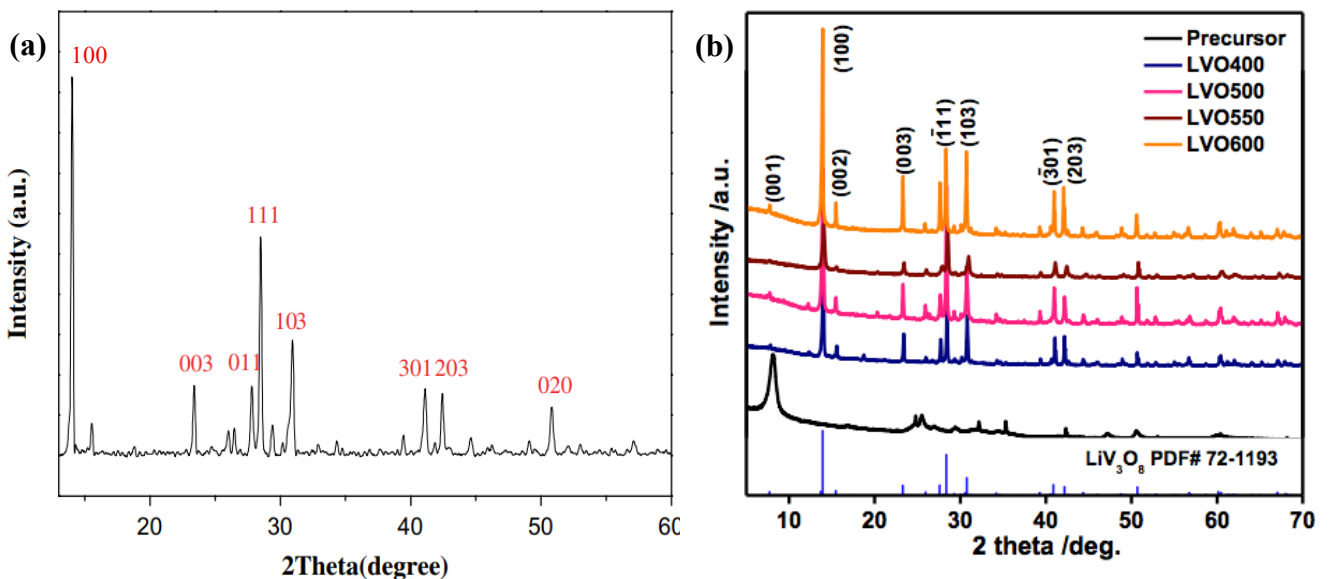

Figure 2.11: XRD pattern of (a) the as-prepared LiV_3O_8 calcined at 550°C for 5 h under air (Liu *et al.*, 2011) and (b) LiV_3O_8 electrodes calcined at different temperatures (Wang, *et al.*, 2016).

The diffraction peak of LiV_3O_8 will change upon cycling. The intensity of the significant peaks in LiV_3O_8 decrease after 100 cycles (Figure 2.12). The pronounced peak, (100) decreases the most after cycling. This is because of Li ion transformation and phase changes occur in LiV_3O_8 structure.
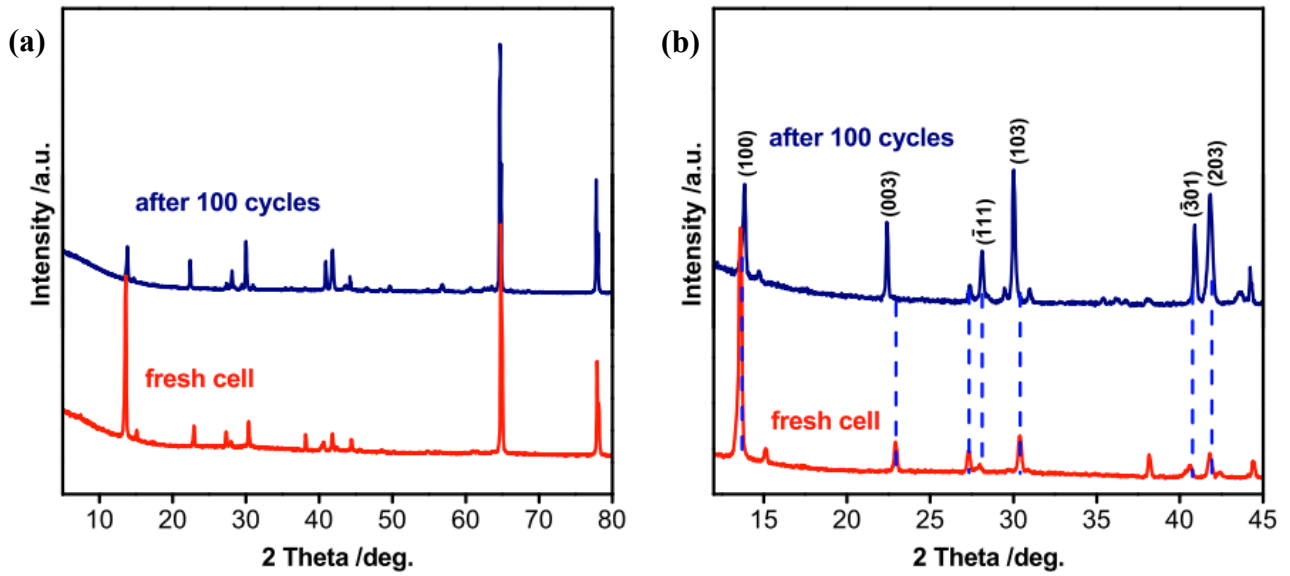

Figure 2.12: XRD comparison: (a) of LVO-600 electrode before cycling and after 100 cycles at applied current density of 60 mAg^{-1} (b) and enlarged pattern (Wang *et al.*, 2016)

2.3.2 Morphological Properties

For the examination of the microstructure morphology and chemical composition characterizations of LiV_3O_8, scanning electron microscope (SEM) is one of the most versatile instruments available. A sample of pristine LiV_3O_8 is shown in Figure 2.13 (a). Rod shape is the most commonly found for the products of the sol-gel method (Liu *et al.*, 2011). It can be seen clearly that LiV_3O_8 in nano-rod is about 2 μm in length and 500 nm in width.
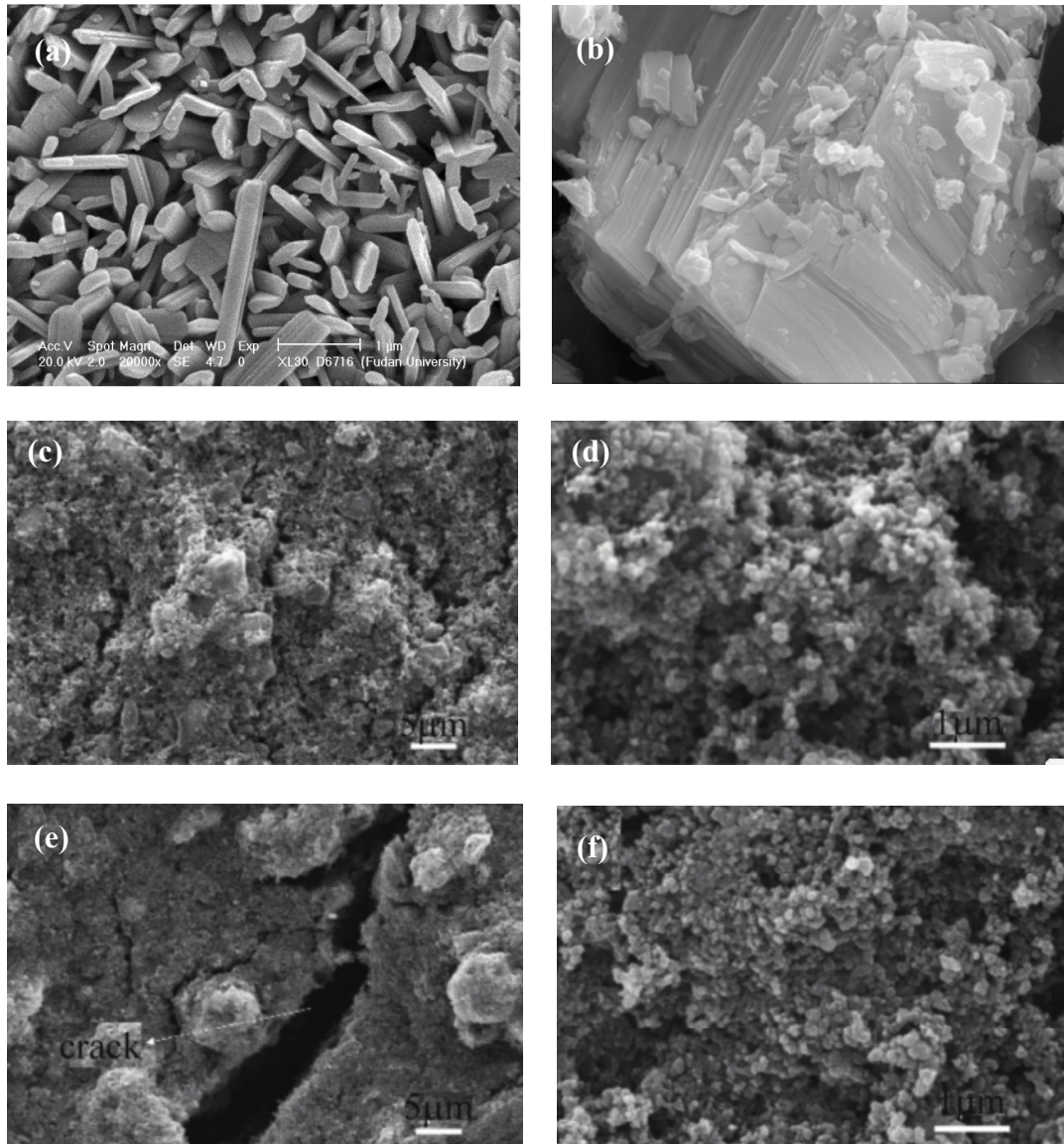
Figure 2.13: SEM of (a) pristine LiV$_3$O$_8$ in nano-rod shape (Liu et al., 2011), (b) magnified pristine LiV$_3$O$_8$ (Zhao et al., 2011) , (c) & (d) oxidized agar as binder in LiV$_3$O$_8$ and (e) & (f) Polyvinylidene fluoride as binder in LiV$_3$O$_8$ after cycling with different magnifications (Tang & Xiong, 2017)

Agar becomes an option as a binder in battery is because of its ability to eliminate liquid from a gel. It could be used to improve mechanical resistance and compaction to the active materials and current collector in the electrode. Agar binder also tends to give the wettability to the surface. It favours the contact between electrolyte and electrode during the process (Liu *et al.*, 2011). In battery, although binder is an electrochemically inactive materials, it also plays an important role on the electrode activity.

Figure 2.13 (e) shows the SEM image of the surface of the lithium sulphur electrode, where a big crack can be seen clearly on the surface of electrode with PVDF binder after 100 cycles. Oxidized Agar improved the adherence of the battery anode (Tang & Xiong, 2017).

2.3.3 Elemental Analysis

Energy dispersive X-ray spectroscopy (EDX) is an analytical technique used for elemental analysis and chemical characterization of LiV_3O_8 electrode. It can be used for analysing the characteristic X-rays generated from the sample after it is bombarded by electrons. The EDX patterns exhibit qualitative and quantitative information on the chemical composition and elements. In addition, EDX mapping illustrates the species distribution near the surface region (Zhang, 2015). Carbon, Vanadates, oxide and fluoride were showed on the surface of LiV_3O_8 electrode (Figure 2.15).